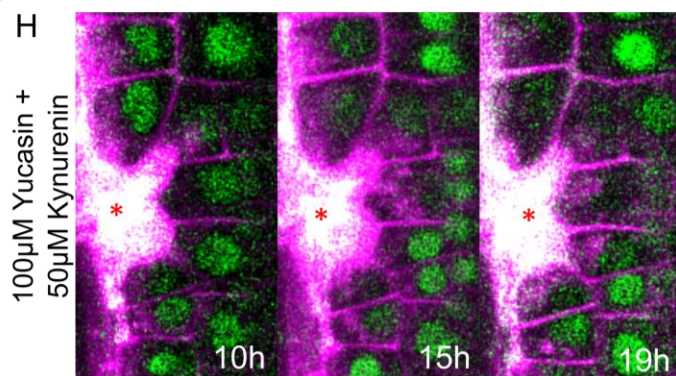
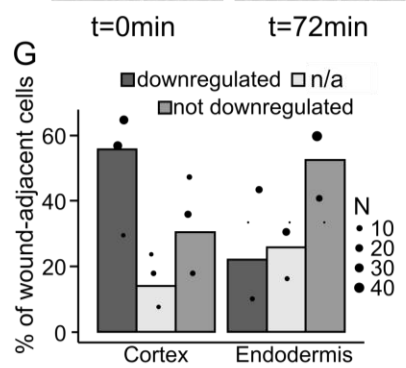
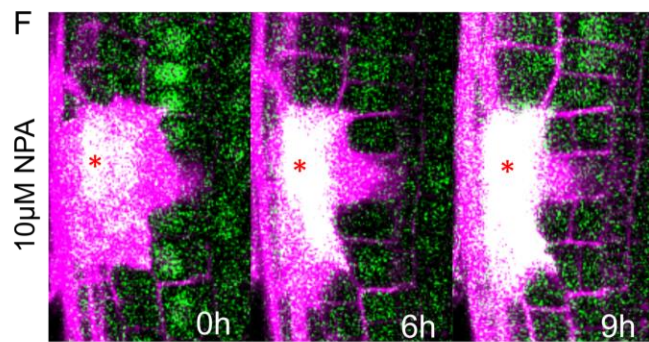
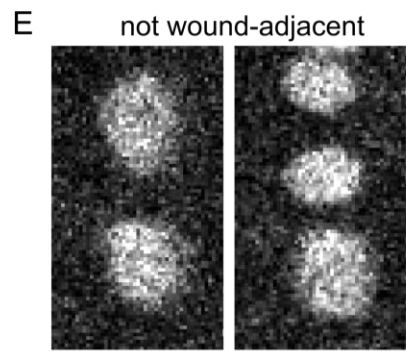
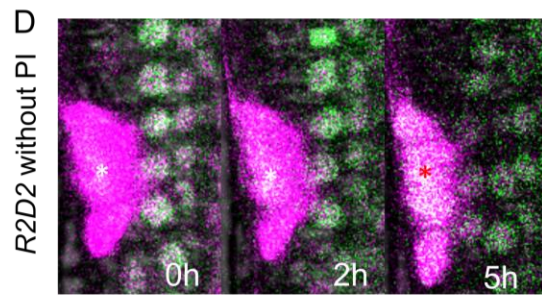
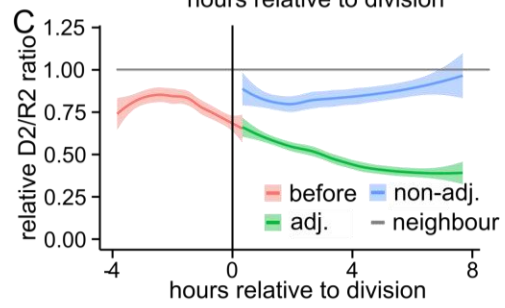
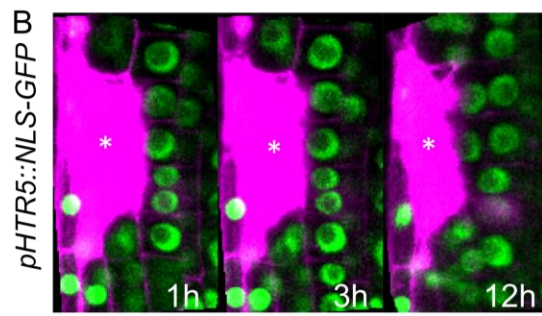
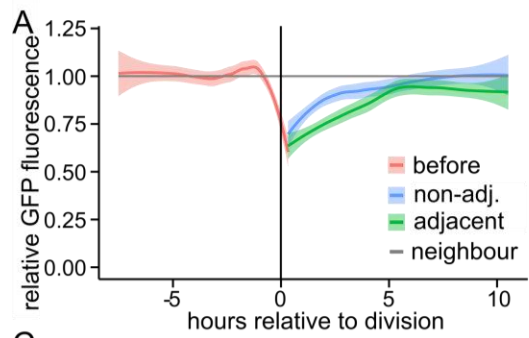


## **SUPPLEMENTARY INFORMATION**

### **Supplementary Figures**



**Figure S1. Downregulation of DII-Venus is specific and occurs only in wound-adjacent cells**

(A-B) The ubiquitously expressed *HTR5::NLS-GFP* is not downregulated in wound-adjacent cells. (A) Quantification of the relative GFP fluorescence (of *HTR5::NLS-GFP*) over time of wound-adjacent cells before (red), or after cell division (wound-adjacent in green; non-wound adjacent in blue). Data are represented as GFP fluorescence in observed cells relative to neighbouring, not-adjacent cells. Time 0 hours represents time of wound-adjacent cell division. Thick lines represent the smoothed mean and lighter background represents smoothed standard error from n=7 cells each. (B) Cells expressing *HTR5::NLS-GFP* (green) in cells next/adjacent to ablated cell (marked with asterisk) at three different times (1, 3 and 12 hours). Notice that intensity is not affected during the progress of regeneration or after the first division.

(C-D) Downregulation in wound-adjacent cells is specific to DII-Venus compared to mDII-ntdTomato. (C) Quantification of the relative DII/mDII (= D2/R2) ratio over time of wound-adjacent cells before (red), or after cell division (wound-adjacent in green; non-wound adjacent in blue). Data are represented as DII/mDII fluorescence intensity ratio in observed cells relative to neighbouring, not-adjacent cells. Time 0 hours represents time of wound-adjacent cell division. Thick lines represent the smoothed mean and lighter background represents smoothed standard error from n=5 cells each. (D) Cells expressing R2D2 marker (green) without PI staining, in cells next/adjacent to ablated cell (asterisk) at three different times after ablation (0, 2 and 5 hours). Notice the downregulation of DII-Venus (green) in wound-adjacent cells before and after the first division.

(E) Non-wounding adjacent cells expressing DII-Venus before (left) and after (right) anticlinal (normal) divisions.

(G) Quantification of percentage of wound-adjacent cortex or endodermal cells with downregulation (black bars), n/a (not measurable; grey bars) or non-downregulation (dark grey bars) of DII-Venus expression during long-term imaging. Data are represented as weighted mean from 3 experiments (bars) and individual values (dots, area indicates sample size).

(F, H) Transport or local synthesis of auxin are not determinant for controlling the upregulation of auxin signalling in the wounding-adjacent cell. DII-Venus (green) expression (of R2D2 negative auxin marker line) in cells around/next/adjacent to ablated cell (marked with asterisk) between 0-19 hours after cell ablation in media supplemented with 10  $\mu$ M NPA (F) or 100  $\mu$ M + 50  $\mu$ M Kynurenine (H). Ablated cells are marked with asterisk.

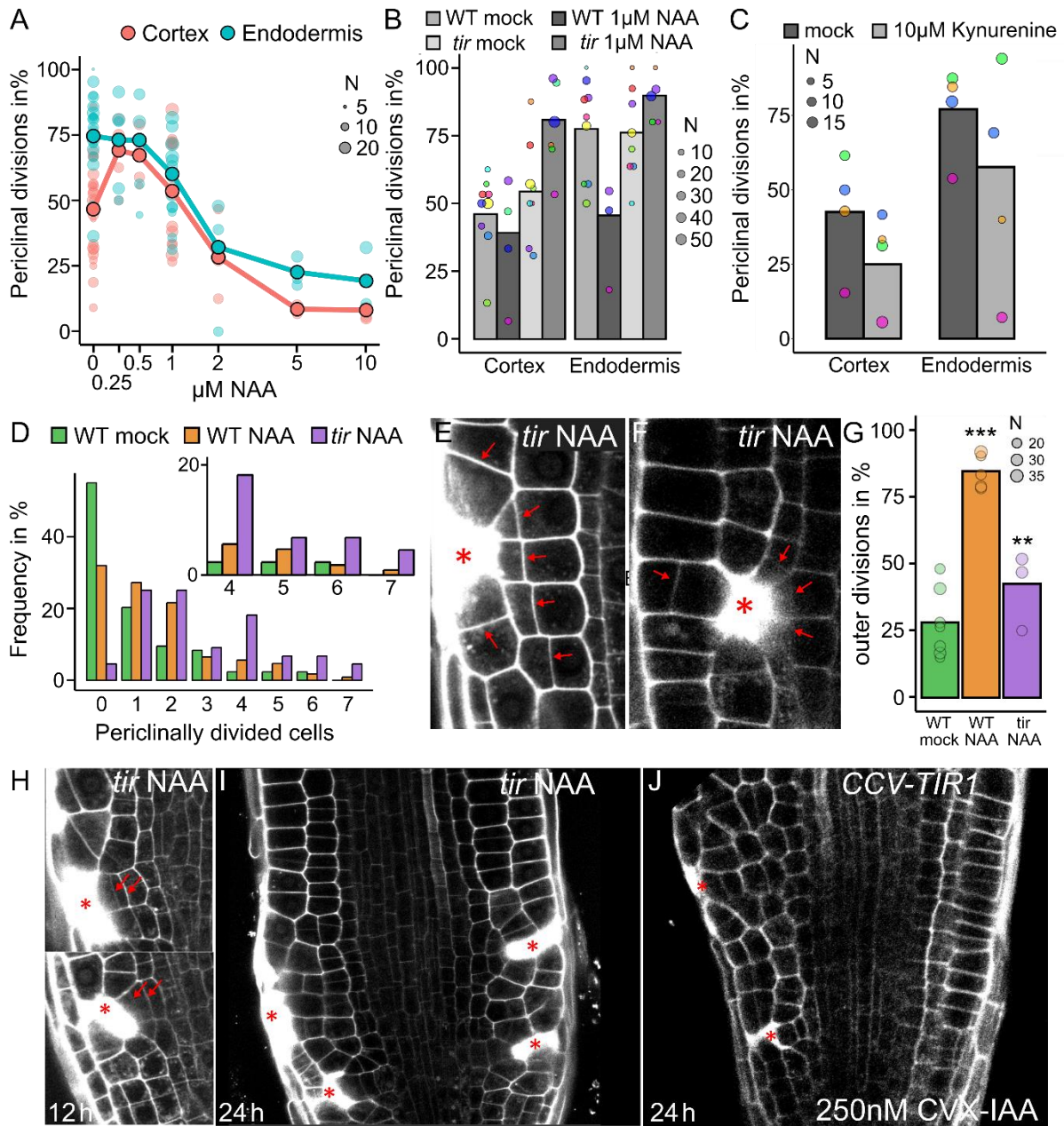


**Figure S2. Auxin effect on restorative divisions and dependency on TIR1 activity**

**(A-B)** Representation of the absolute division rates from Fig. 2A and 2B as number of periclinal divisions 12 hours after ablation. **(A)** Restorative periclinal division rates (in %) of endodermal (blue) and cortex (red) cells, after different auxin (NAA, from 0 to 10  $\mu$ M) concentration application. Big dots represent weighted mean and lighter dots represent individual experiments (area indicates sample size). **(B)** Restorative periclinal divisions rate (in %) of cortex and endodermal cells of Wt and *tir triple* mutant plants on mock and upon 1  $\mu$ M NAA treatments. Data are represented as weighted mean (bar) and individual experiments (dots, area indicates sample size).

**(C)** Restorative periclinal divisions rate (in %) of cortex and endodermal cells during mock and 10  $\mu$ M Kynurenine treatments. Data are represented as weighted mean (bar) and individual experiments (dots, area indicates sample size).

**(D-G)** Auxin expands zone of wound-responsive divisions in Wt and *tir triple* plants. **(D)** Quantification of the number of inner adjacent cells undergoing periclinal divisions from Wt mock treated (green), Wt 1 $\mu$ M NAA treated (orange) and *tir triple* 1 $\mu$ M NAA treated (violet) plants. Data are represented as frequency of the respective amount of divisions. **(E)** Restorative cortex divisions in 1  $\mu$ M NAA treated *tir triple* plants after epidermal cell ablation (asterisk). **(F)** Restorative cell divisions in outer epidermis cells in 1  $\mu$ M NAA treated *tir triple* plants after epidermal cell ablation (asterisk). **(G)** Quantification of the number of outer adjacent cells undergoing periclinal divisions from Wt mock treated (green) Wt 1 $\mu$ M NAA treated (orange) and *tir triple* 1  $\mu$ M NAA treated (violet) plants. Data are represented as weighted mean (bar) and individual experiments (dots, area indicates sample size).

**(H)** Double restorative divisions in 1  $\mu$ M NAA treated *tir triple* plants 12 hours after ablation.

**(I-J)** Root-swelling inducing restorative cell divisions in 1  $\mu$ M NAA treated *tir triple* plants **(I)** and in 250 nM CVX-IAA treated *CCV-TIR1* plants **(J)** 24 hours after ablation.

Red arrows indicate new, oblique-periclinal cell plates.



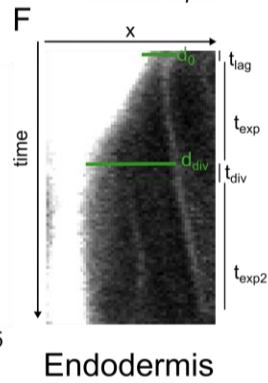
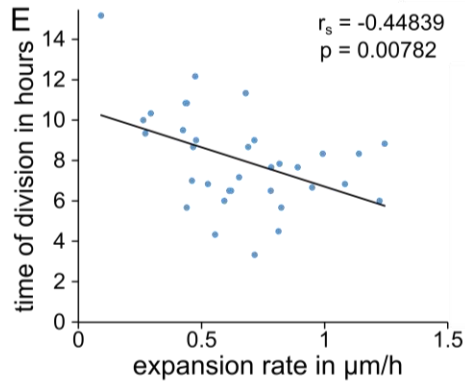
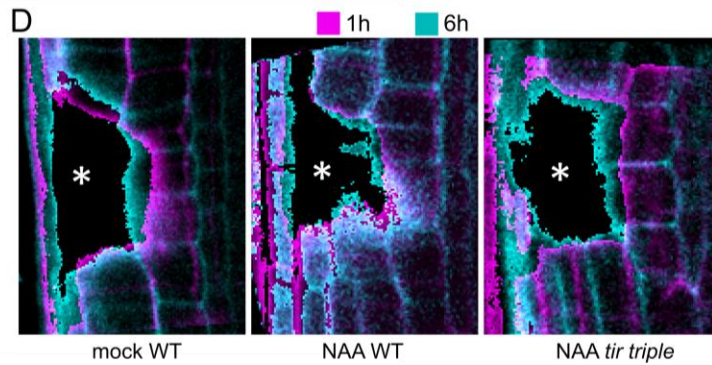
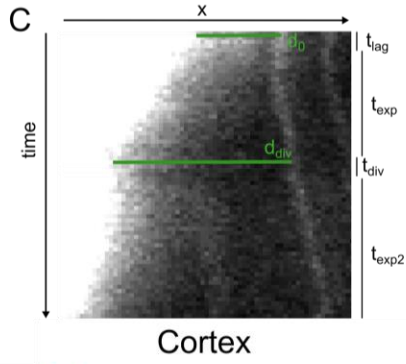
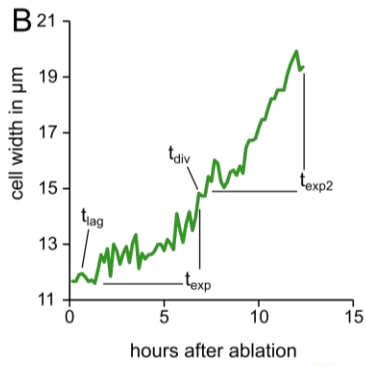
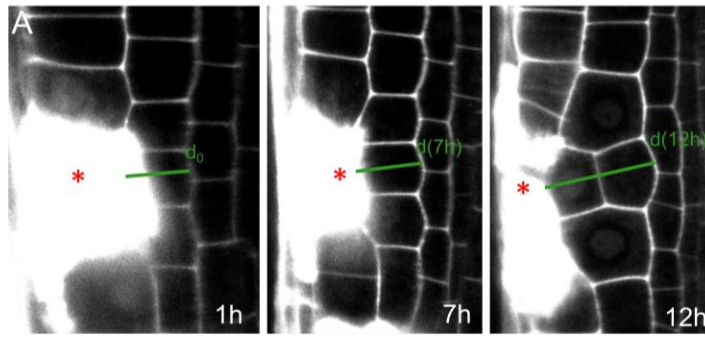


### **Figure S3. Wound-responsive cell expansion in cortex cells**

**(A-D)** Pre-mitotic expansion in cortex cells similar to endodermal cells (Fig. 3). **(A)** Cell expansion dynamics of a cortex cell during wounding (epidermis cell ablated, asterisk). Wound-induced cell expansion in cortex 1 hour after cell ablation (left panel), after 7 hours (middle panel) or after cell division (12 hours, right panel). **(B)** Representation of the cell width (in  $\mu\text{m}$ ) of one representative cortex cell during the restorative cell division stages (in hours after ablation). **(C)** Kymograph of the expansion of the cortex cell from Fig. S3B. The cell width is represented as the distance between the ablated epidermis cell (white area on the left) and the inner neighbour (grey line on the right). The duration of the lag, expansion, division and second expansion phase are indicated on the right. **(D)** Overlay of wound-adjacent cell width of cortex cells at two different time points (1 hour in magenta, and 6 hours in cyan) after ablation in Wt roots on mock (left panel) or upon 1  $\mu\text{M}$  NAA treatment (middle panel), or in 1  $\mu\text{M}$  NAA treated *tir* triple roots (right panel). Asterisk marks ablated cell. **(E)** Representation of the correlation between pre-mitotic expansion rates and the time required for restorative divisions. The Spearman correlation ( $r_s$ ) and the statistical significance (p-value) are indicated in the top right corner. **(F)** Kymograph of the expansion of the endodermal cell from Fig. 3B. The cell width is represented as the distance between the ablated cortex cell (white area on the left) and the inner neighbour (grey line on the right). The duration of the lag, expansion, division and second expansion phase are indicated on the right.

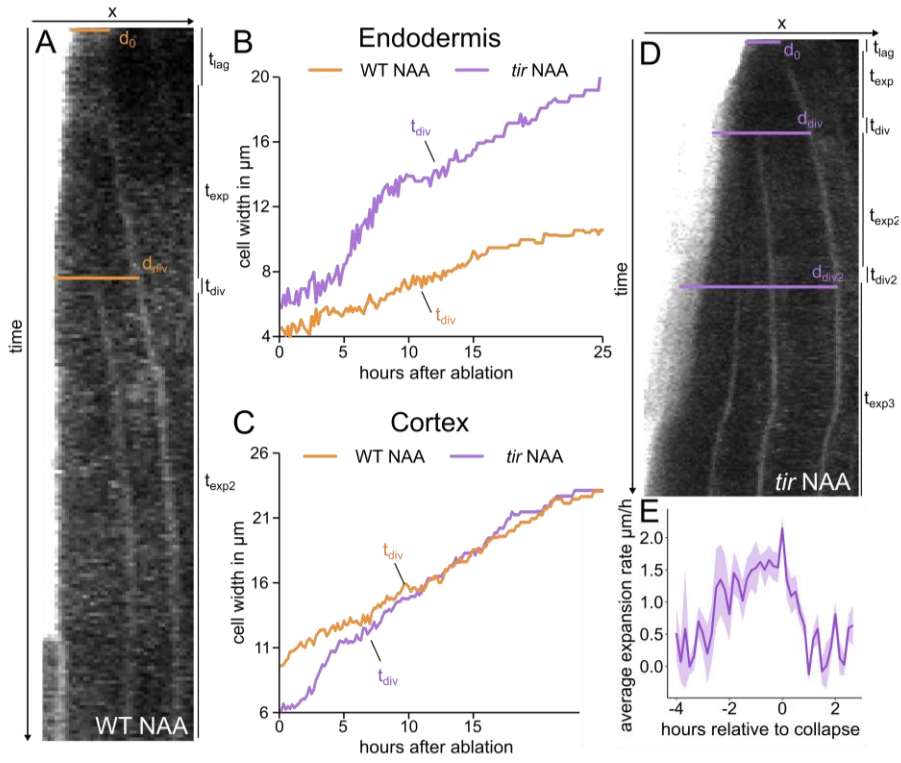




#### **Figure S4. Wound-responsive cell expansion during auxin treatment**

**(A-D)** Auxin promotes cell expansion in *tir triple* plants and inhibits in Wt plants. **(A)** Kymograph of the 1  $\mu$ M NAA treated Wt endodermal cell in Fig. S4B. The cell width is represented as the distance between the ablated cortex cell (white area on the left) and the inner neighbour (grey line on the right). Note that the cell width increase and first division are significantly delayed. **(B-C)** Representation of the cell width (in  $\mu$ m) over time in Wt NAA (orange) and *tir triple* NAA (violet) samples from representative endodermal (B) and cortex (C) cells. **(D)** Kymograph of the 1  $\mu$ M NAA treated *tir triple* cortex cell in Fig. S4C. Note that cell expansion and first division are significantly accelerated resulting in a second division and a third expansion phase.

**(E)** Representation of the cell expansion collapse in 1  $\mu$ M NAA treated *tir triple* plants. Expansion rates are plotted as mean of N=5 cells (thick line) with standard error (light background). Note that fast expansion followed by collapse can be observed also in violet lines of Fig. S4B and C.

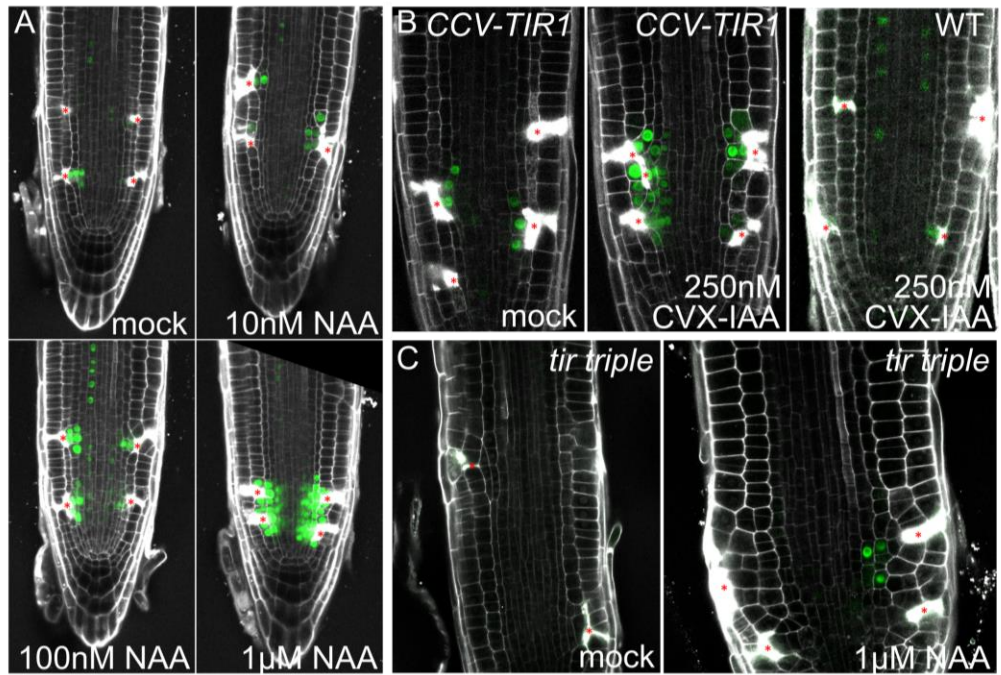


**Figure S5. ERF115 expression depends on auxin concentration and TIR1 activity.**

(A) *ERF115::GFP* (green) expression on wound-adjacent cells on mock or upon 10 nM, 100 nM or 1  $\mu$ M NAA treatments 12 hours after ablation.

(B) *ERF115::GFP* (green) expression on wound-adjacent cells in the *CCV-TIR* background with mock (left) or 250 nM CVX-IAA treatment (middle) compared to CVX-IAA treated Wt plants (right) 12 hours after ablation.

(C) *ERF115::GFP* (green) expression on wound-adjacent cells in mock (left) and 1  $\mu$ M NAA treated (right) *tir triple* samples 24 hours after ablation.

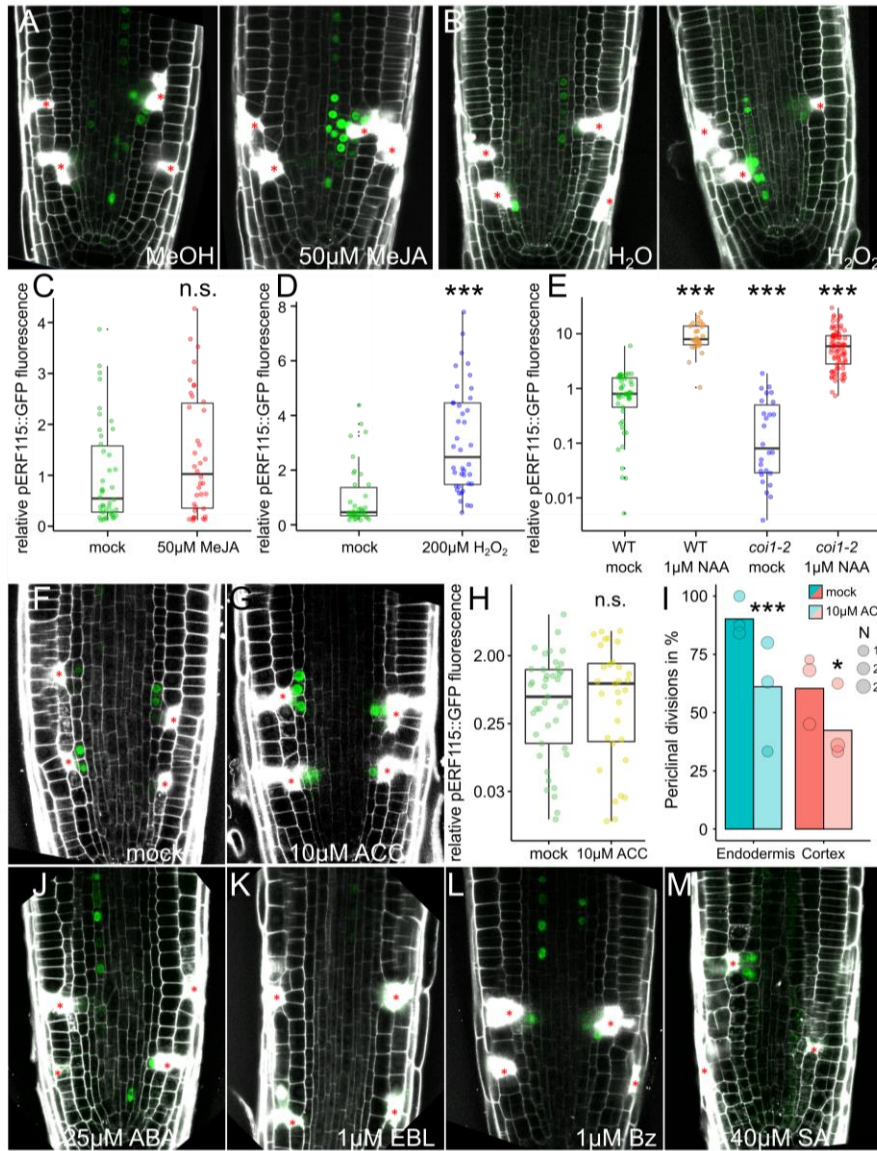


**Figure S6. Effects of known regulators and wound hormones on ERF115 expression**

**(A, C)** MeJA treatment slightly increases ERF115 expression after wounding. **(A)** *ERF115::GFP* (green) expression on wound-adjacent cells in mock (MeOH) and 50  $\mu$ M MeJA treated plants 12 hours after ablation. **(C)** Quantification of the relative *ERF115::GFP* fluorescence in wound-adjacent cells (normalized to the *ERF115::GFP* mean intensity on mock conditions), on mock conditions (green dots) or upon 50  $\mu$ M MeJA treatment (red dots). Data are represented as relative fluorescence intensities of individual cells. Statistical significance was computed from a two-sample Wilcoxon test.

**(B, D)** H<sub>2</sub>O<sub>2</sub> treatment increases ERF115 expression after wounding. **(B)** *ERF115::GFP* (green) expression on wound-adjacent cells in mock (H<sub>2</sub>O) and 200  $\mu$ M H<sub>2</sub>O<sub>2</sub> treated plants 12 hours after ablation. **(D)** Quantification of the relative *ERF115::GFP* fluorescence in wound-adjacent cells (normalized to the *ERF115::GFP* mean intensity on mock conditions), on mock conditions (green dots) or upon 200  $\mu$ M H<sub>2</sub>O<sub>2</sub> treatment (blue dots). Data are represented as relative fluorescence intensities of individual cells. Statistical significance was computed from a two-sample Wilcoxon test.

**(E)** Quantification of the relative *ERF115::GFP* fluorescence in wound-adjacent cells (normalized to the *ERF115::GFP* mean intensity on mock conditions), in Wt on mock conditions (green dots) and upon 1  $\mu$ M NAA treatment (orange dots) or in *coil-2* mutant plants (blue and red dots, respectively). Data are represented as relative fluorescence intensities of individual cells on a logarithmic scale. Statistical significance was computed from a two-sample Wilcoxon test.

**(F-I)** Ethylene does not enhance ERF115 expression or restorative division rates. *ERF115::GFP* (green) expression in wound-adjacent cells upon mock **(F)** and 10 $\mu$ M ethylene precursor ACC **(G)**. **(H)** Quantification of the relative *ERF115::GFP* fluorescence in wound-adjacent cells (normalized to the *ERF115::GFP* mean intensity on mock conditions), on mock conditions (green dots) or upon 10  $\mu$ M ACC treatment (yellow dots). Data are represented as relative fluorescence intensities of individual cells. Statistical significance was computed from a two-sample Wilcoxon test. **(I)** Restorative periclinal divisions rate (in %) of cortex and endodermal cells during mock and 10  $\mu$ M ACC treatments. Data are represented as weighted mean (bar) and individual experiments (dots, area indicates sample size). Statistical significance was computed conditional logistic regression.

**(J-M)** *ERF115::GFP* (green) expression in wound-adjacent cells upon 25  $\mu$ M ABA (**J**), 1  $\mu$ M EBL (**K**), 1  $\mu$ M Bz (**L**) or 40  $\mu$ M SA treatment (**M**) 12 hours after ablation.

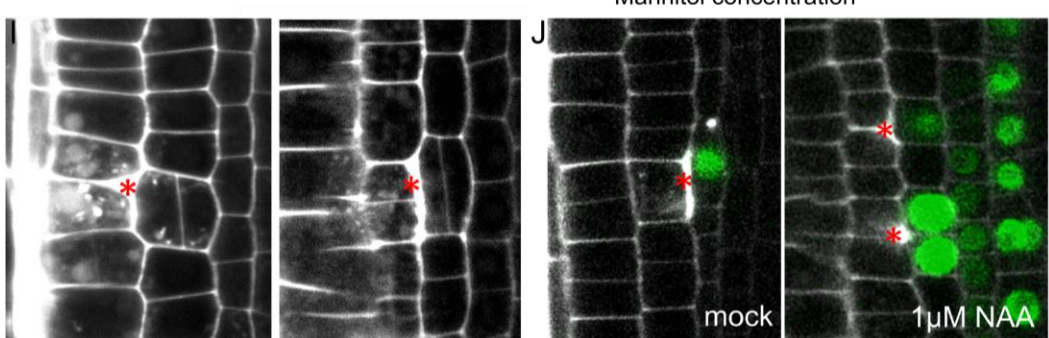
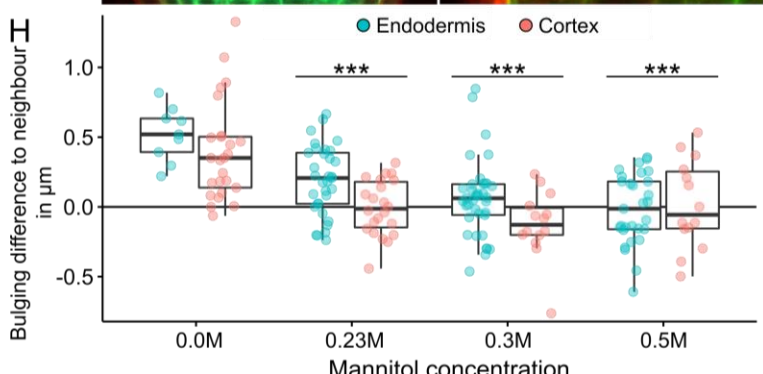
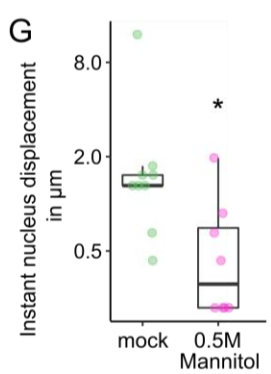
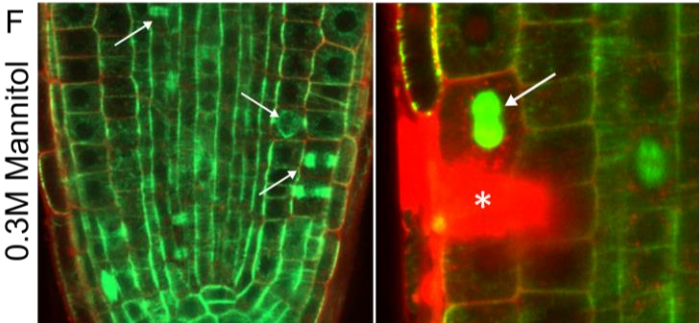
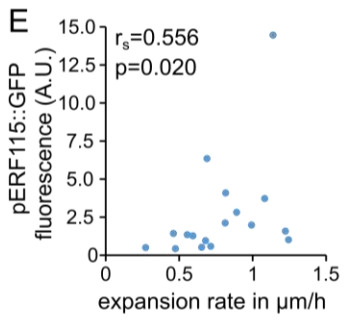
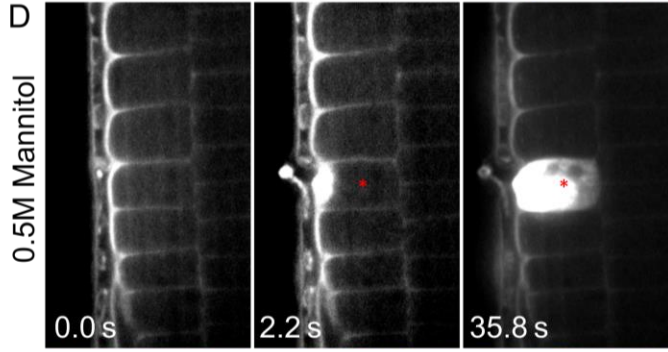
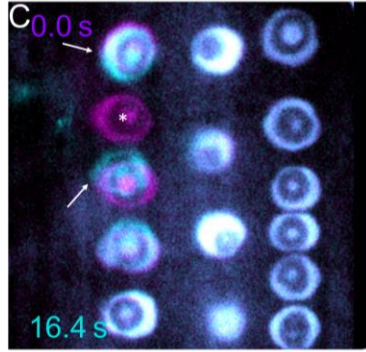
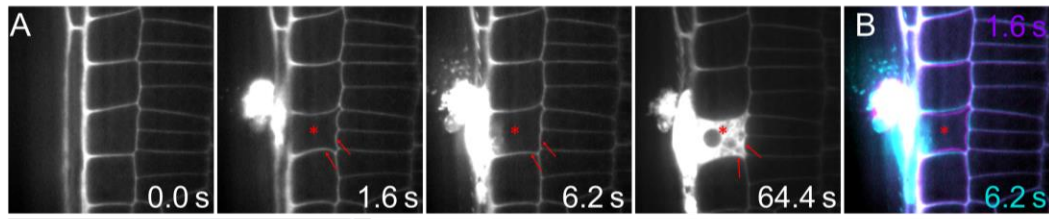




### Figure S7. Wound-triggered changes in tissue pressure

**(A-B)** Ablation of a single cell causes release of cellular content and a reduction of turgor pressure in neighbouring cells. **(A)** Short term responses of ablated cells (asterisk) and their neighbours before ablation (0.0 s) and directly afterwards (1.6 s, 6.2 s and 64.4 s, from left to right). Released cellular content after ablation can be seen in white and red arrows mark neighbouring cell wall. Note that neighboring cell walls bulge immediately after ablation, retract afterwards and become bulged again after later time. **(B)** Overlay of two time points (1.6 s in magenta, and 6.2 s in cyan) after ablation (asterisk) showing the retraction of bulging of the neighbouring cells.

**(C)** Overlay of two time points (0 s in magenta, and 16.4 s in cyan) showing the displacement of nuclei in neighbouring cells (white arrows) after ablation of a single cell (asterisk).

**(D)** Short term responses of ablated cells (asterisk) and their neighbours before ablation (0.0 s) and directly afterwards (2.2 s, and 35.8 s, from left to right) upon 0.5 M Mannitol treatment. Note that release of cellular content and bulging are absent.

**(E)** Representation of the correlation between pre-mitotic expansion rates and *ERF115::GFP* fluorescence at the time of division. The Spearman correlation ( $r_s$ ) and the statistical significance (p-value) are indicated in the top left corner.

**(F)** Anticlinal divisions are marked by *35S::MAP4-GFP* (green) stained spindles (white arrows) during hyperosmotic treatment (0.3 M Mannitol) in PI stained (red), undisturbed (left) and wound-adjacent cells (right, asterisk marks ablation).

**(G)** Representation of nucleus displacement immediately (max. 5 seconds) after ablation in cells upon mock (green) or 0.5M Mannitol treatment (purple). Note that nucleus displacement, i.e. cellular burst and collapse are merely absent from Mannitol treated samples. Statistical significance was computed from a two-sample Wilcoxon test.

**(H)** Turgor pressure driven bulging in wound adjacent cells is reduced upon Mannitol treatment. **(H)** Representation of the difference between bulging in wound adjacent to non-adjacent cells in endodermis (blue) and cortex cells (red) upon different mannitol concentration treatments. The distance of the bulging from inner neighbours (red) is subtracted from reference, non-adjacent cells (grey), resulting in positive (more bulging than in neighbours) or negative values (less bulging than neighbours). Statistical significance between 0.0M (mock) and the respective mannitol treatment was calculated from a two-sample Wilcoxon test.

**(I)** Periclinal cell divisions after harming the cell envelope between epidermis and cortex (left) or cortex and endodermis (right).

**(J)** *ERF115::GFP* expression after harming the cell envelope between cortex and endodermis in untreated (left) but or in 1  $\mu$ M NAA treated plants (right)

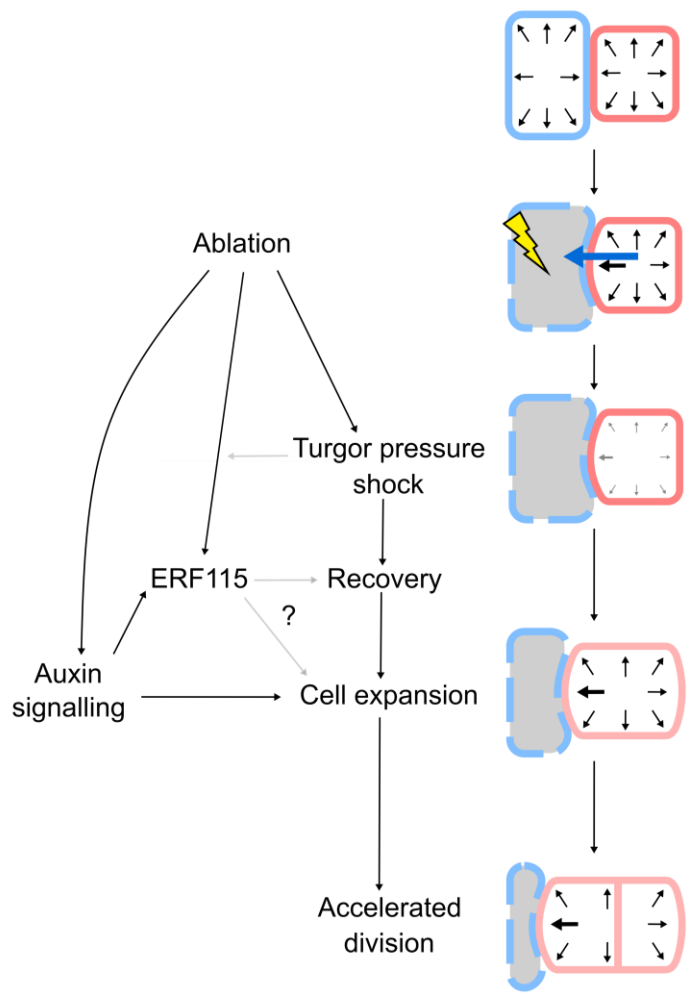


**Figure S8. Schematic summary of auxin effects on cell expansion, ERF115 expression and division rates**

Black arrows indicate turgor pressure driven forces on the cell wall, while a blue arrow indicates the loss of cellular content. A lighter colour of the cell wall indicates a presumable modification of the cell wall properties. The timeline of events runs from top to bottom.

## **Supplementary movie legends**

### **Movie S1. DII-Venus-visualized auxin signalling in wound-adjacent cells**

Time-lapse movie of R2D2 (DII-Venus in green) stained with PI (pink) during regeneration of a single cell ablation. For further details, see Fig. 1

### **Movie S2. Ubiquitously expressed nuclear GFP in wound adjacent cells**

Time-lapse movie of *HTR5::NLS-GFP* (green) stained with PI (pink) during regeneration of a single cell ablation. For further details, see Fig. S1

### **Movie S3. DII-Venus and mDII-ntdTomato-visualized auxin signalling in wound-adjacent cells**

Time-lapse movie of R2D2 (DII-Venus in green, mDII-ntdTomato in pink) during regeneration of a single cell ablation. Notice the strong bleaching of overall fluorescence throughout the movie. For further details, see Fig. S1

### **Movie S4. DII-Venus-visualized auxin signalling during inhibited polar auxin transport in wound-adjacent cells**

Time-lapse movie of R2D2 (DII-Venus in green) stained with PI (pink) during regeneration of a single cell ablation treated with 10  $\mu$ M NPA. Notice the strong auxin accumulation during NPA treatment. For further details, see Fig. S1

### **Movie S5. DII-Venus-visualized auxin signalling during inhibited auxin biosynthesis in wound-adjacent cells**

Time-lapse movie of R2D2 (DII-Venus in green) stained with PI (pink) during regeneration of a single cell ablation treated with 100  $\mu$ M + 50  $\mu$ M Kynurenine. Notice the delayed induction of divisions. For further details, see Fig. S1

### **Movie S6. Wound-responsive cell expansion in endodermal cells**

Time-lapse movie of PI stained (grayscale) endodermis cells after ablation of a cortex cell during cell expansion and restorative divisions. These are the cells quantified in Fig. 3B.

## Movie S7. Wound-triggered changes in tissue pressure

Time-lapse movie of PI stained (grayscale) ablation of a single epidermis cells and the subsequent pressure changes in the surrounding tissues. For further details, see Fig. S7.

### Supplementary Codes

#### Code 1. Statistical evaluation of binary data with Conditional Logistic Regression

```
>library(survival)
>library(readxl)

>#provide data in df_test as in the following format:
># header: sample|exp|PD|ablated|type
># rows: name of sample (e.g.:"mock")|No. of repetition|No. of positive events (periclinal
divisions)|No. of observed events (ablations)

>typ="endodermis" #type in cell type you want to observe
>test="treatment" #your test sample
>ctrl="mock" #your control sample

>#building of a dataframe with each observed event (each ablation, here called "cell") as a
separate row (with incrementing numbers)
>df_test_test=df_test[df_test$sample == ctrl | df_test$sample == test,]
>df_test_test=df_test_test[df_test_test$type ==typ,]

>data1=as.data.frame(1:sum(df_test_test$ablated))
>colnames(data1)="cell"

>#each event gets assigned its respective repetition ("exp")
>exp=NULL
>for (i in 1:max(df_test$exp)) {
> exp=c(exp, rep(i,sum(df_test_test[df_test_test$exp==i,]$ablated)))
>}
>data1=cbind(data1,exp=exp)

>#each event gets assigned a binary value whether it triggered a positive (1, here a "PD") or a
negative (0, here "no PD") event
>PD=NULL
>for (i in 1:max(df_test$exp)) {
> PD=c(PD, rep(1,df_test_test[df_test_test$exp==i & df_test_test$sample==test ,]$PD),
rep(0,df_test_test[df_test_test$exp==i & df_test_test$sample==test ,]$ablated-
```

```

df_test_test[df_test_test$exp==i & df_test_test$sample==test
,]$PD),rep(1,df_test_test[df_test_test$exp==i & df_test_test$sample==ctrl ,]$PD),
rep(0,df_test_test[df_test_test$exp==i & df_test_test$sample==ctrl ,]$ablated-
df_test_test[df_test_test$exp==i & df_test_test$sample==ctrl ,]$PD))
>}
>data1=cbind(data1,PD=PD)

>#each event gets assigned a binary value whether it is a control sample (0, here" "not mut")
or test sample (1, here a "mut" for mutant)
>mut=NULL
>for (i in 1:max(df_test$exp)) {
> mut=c(mut, rep(1,df_test_test[df_test_test$exp==i & df_test_test$sample==test
,]$ablated), rep(0,df_test_test[df_test_test$exp==i & df_test_test$sample==ctrl ,]$ablated))
>}
>data1=cbind(data1,mu=mut)

>#calculation considering each experiment individually (conditional)
>model <- clogit(data=data1, PD ~ mut + strata(exp))
>summary(model)

```